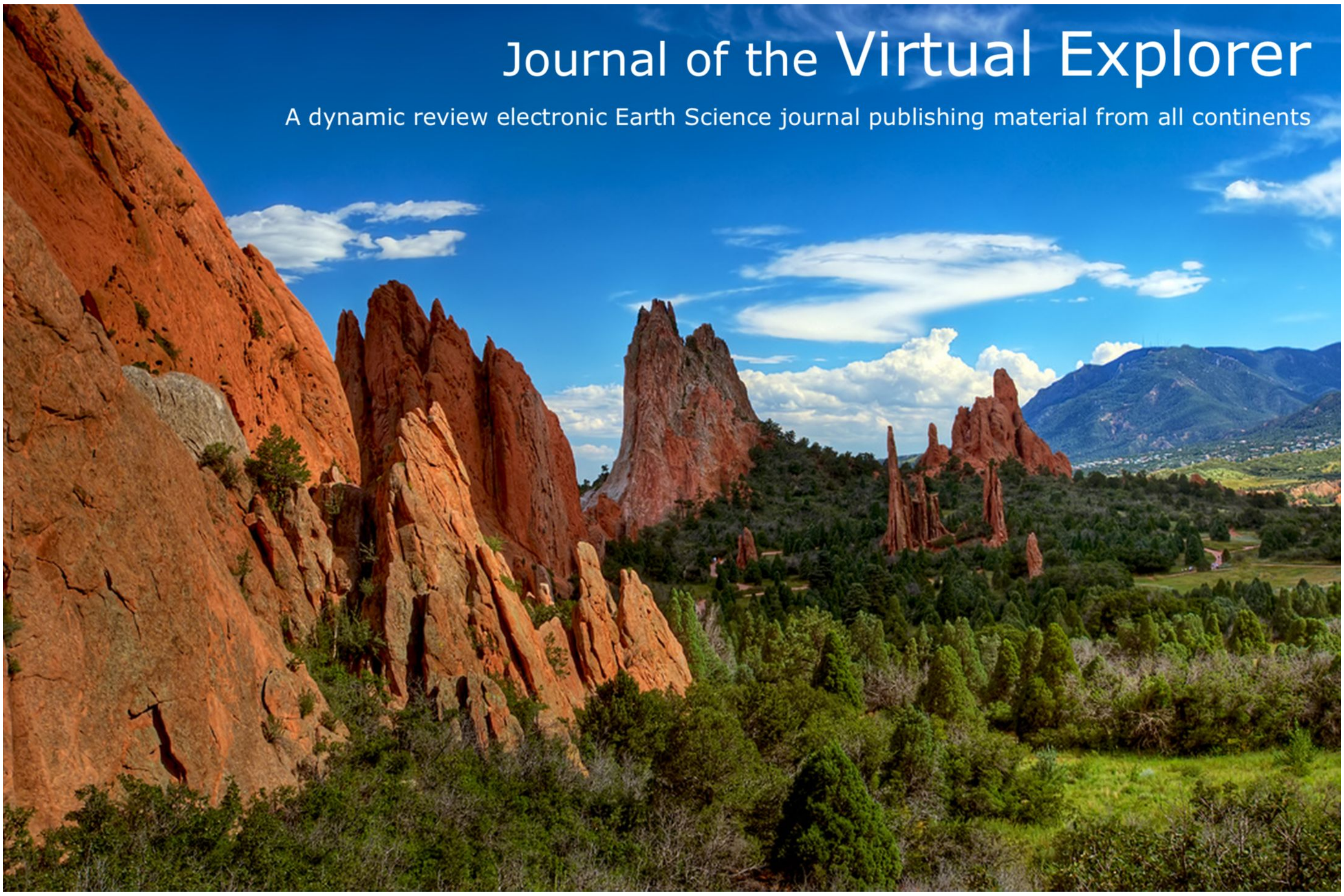

Tectonomagmatic evolution of the Bastar craton of Indian shield through plume-arc interaction: evidence from geochemistry of the mafic and felsic volcanic rocks of Sonakhan greenstone belt

Md. Erfan Ali Mondal, Mahshar Raza

Journal of the Virtual Explorer, Electronic Edition, ISSN 1441-8142, volume **32**, paper 7
In: (Eds.) Talat Ahmad, Francis Hirsch, and Punya Charusiri,
Geological Anatomy of India and the Middle East, 2009.

Tectonomagmatic evolution of the Bastar craton of Indian shield through plume-arc interaction: evidence from geochemistry of the mafic and felsic volcanic rocks of Sonakhan greenstone belt

Md. Erfan Ali Mondal, Mahshar Raza

Journal of the Virtual Explorer, Electronic Edition, ISSN 1441-8142, volume **32**, paper 7
In: (Eds.) Talat Ahmad, Francis Hirsch, and Punya Charusiri,
Geological Anatomy of India and the Middle East, 2009.

Abstract: The Sonakhan Group of Bastar craton of the central Indian shield comprises volcano-sedimentary rocks. The lower part of this belt, referred to as Baghmara Formation, consists of two distinct units of volcanic associations: (1) the lower unit consisting entirely of mafic volcanic rocks of basaltic composition and (2) the upper unit comprising volcanic rocks of basalt-andesite-dacite-rhyolite (BADR) series. The geochemical characteristics of the lower unit basalts include tholeiitic nature with depletion in highly incompatible elements, Nb-maxima (Nb/Nb* = 0.93-1.48, relative to Th and La) and near flat rare earth element patterns. These metabasalts are distinguished as plume-related oceanic plateau basalt. The upper unit volcanic rocks are mafic, intermediate to felsic in composition with island arc geochemical signatures including enrichment in highly incompatible elements, large negative high field strength element anomalies, depletion of Nb (Nb/Nb* = 0.10-0.68) relative to Th and La and light rare earth element enrichment patterns. Field relationships in combination with geochemical characteristics of the Sonakhan Group reveal the co-existence of plume generated oceanic plateau basalts and island arc related volcanic rocks. It is proposed that the geodynamic evolution of Sonakhan greenstone belt initiated with the formation of a plume generated thickened, hot, buoyant oceanic plateau. This plateau served as a base for subduction of oceanic crust at its margin producing subduction-related mafic and felsic melts in an island arc setting. Our study reveals that Sonakhan greenstone belt of Bastar craton evolved by plume-arc interaction.

Citation: Mondal, M., Raza, M. 2009. Tectonomagmatic evolution of the Bastar craton of Indian shield through plume-arc interaction: evidence from geochemistry of the mafic and felsic volcanic rocks of Sonakhan greenstone belt. In: (Eds.) Talat Ahmad, Francis Hirsch, and Punya Charusiri, *Journal of the Virtual Explorer*, volume **32**, paper 7, doi: 10.3809/jvirtex.2009.00245

Introduction

The Neoarchaean to Paleoproterozoic period is characterized by major crustal formation in the geological history of the Earth (Puchtel *et al.*, 1999). The juvenile crusts formed during this period are preserved within many greenstone belts. Geochemical studies of these greenstone belts have revealed contrasting and diverse rock types (Puchtel *et al.*, 1999; Sandeman *et al.*, 2006; Van Boening and Nabelek, 2008; Polat, 2009 and reference therein) indicating diversity and complexity in the crust formation and evolutionary processes. In the last two decades, the island arc model has been the most popular mechanism describing the formation of the continental crust. But during the 1990s, based on strong geochemical database, the plume model was proposed for the origin and growth of many continental nuclei (Stein and Goldstein, 1996; Galer and Mezger, 1998). Mantle plumes generated large amount of basaltic melts rather rapidly in the oceans, and also on the continents, creating plateaus. The oceanic plateaus may accrete laterally to the continents producing new continental fragments (Abbott *et al.*, 1997; Desrochers *et al.*, 1993). Recent geochemical studies of many greenstone belts point to yet another model, the plume-arc accretion model, for the formation and evolution of the crust (Dostal and Muller, 2004; Polat *et al.*, 2005; Polat and Hofmann, 2003, Dostal *et al.*, 2004; Manikyamba *et al.*, 2004; Polat, 2009). This model envisages that many Precambrian greenstone belts which were formed in an intra-oceanic environment show spatial and temporal co-existence of hotspot related and subduction related rocks. Although, apparently contradictory, this mechanism seems to have played an important role in the generation and evolution of Neoarchaean to Paleoproterozoic crust. Large amounts of geochemical data have been growing, especially over the last decade, in favour of this model.

In this contribution, we present major and trace element data, including rare earth elements of the Sonakhan greenstone belt of Bastar craton, central Indian shield, with a view to placing constraints on magma type(s) and source composition of the mafic and felsic volcanic rocks in the light of modern tectonomagmatic concepts. The geochemical data, in combination with field evidence, will be used to develop a comprehensive model for the Neoarchaean to Paleoproterozoic continental growth of the Indian shield.

Geological Setting

The Indian plate is a mosaic of five major nuclei viz. Aravalli-Bundelkhand, Bastar, Western Dharwar, Eastern Dharwar and Singhbhum along with southern granulite terrane (Naqvi and Rogers, 1987). Although stabilization of these nuclei has taken place at different times in the Archaean, a stable configuration of the Indian plate, consisting of all these cratonic blocks, was by and large complete by 2.5 Ga (Stein *et al.*, 2004). The subsequent Paleoproterozoic evolution of the Indian landmass has generally been considered to be the fast accretion of island-arc systems and the formation of the accretionary orogens along the margins of these nuclei.

The Bastar craton of the central Indian shield is bounded by the Eastern Ghats, the Mahanadi and the Godavari rifts and the Son-Narmada lineament. It consists predominantly of gneisses and granitoids with supracrustal rocks viz. Dongargarh, Sakoli, Sukma, Bengpal and Bailadila Iron ore formations. These rocks are overlain by the undeformed Proterozoic basins, referred to as Purana basins (Crookshank, 1963; Naqvi and Rogers, 1987; Ramakrishnan, 1990; Prasad, 1990). In addition to these rocks, the craton contains greenstone belts, which occur as small isolated outcrops near Bastar, Jeypore, Bijapur, Sonepur and Sonakhan (Fig. 1). Bastar craton is the least studied terrain among the cratons of the Indian plate, and so also its greenstone belts. Details of the geological and geochemical studies of these greenstone belts are warranted to unravel the geological evolution of the Indian Precambrian shield. Although the petrological and the tectonic account of the Neoarchaean mafic rocks of the southern Bastar greenstone belt have been carried out by Srivastava *et al.* (2004), Srivastava and Singh (1999) and Srivastava and Verma (1998), no geochemical data are available for the Sonakhan greenstone which lies at the northeastern part of the Bastar craton.

Figure 1. Geological map of the Bastar craton

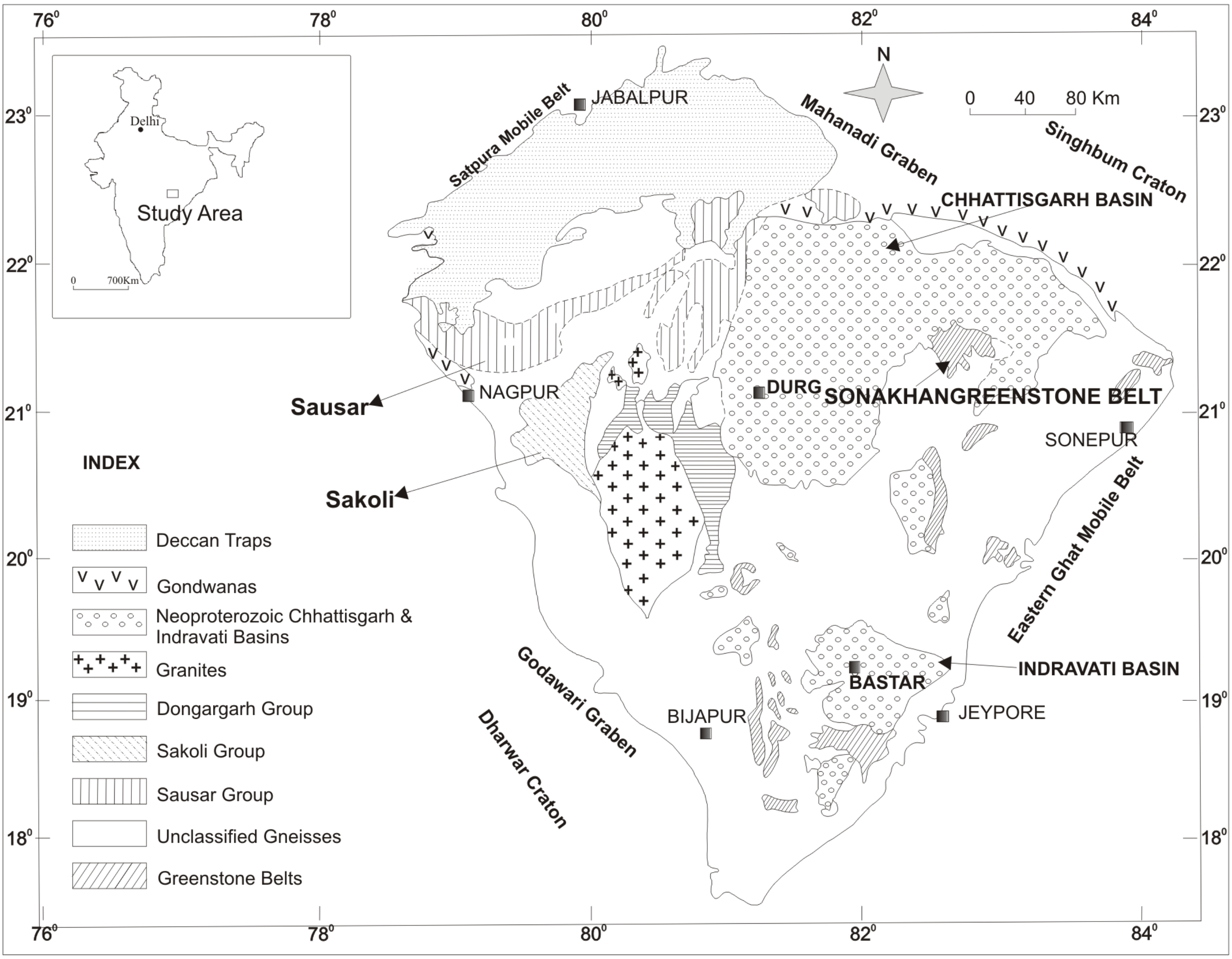

Geological map of the Bastar craton, central Indian shield (Ramakrishnan, 1990), showing locations of the Sonakhan and other greenstone belts. Inset: Map showing the location of the study area.

No radiometric age data are available for the Sonakhan greenstone belt. However, the Sonakhan greenstone belt has been considered equivalent to Neoarchaean to Paleoproterozoic greenstone belts of the southern Bastar craton (Das *et al.*, 1990; Srivastava *et al.*, 2009, 2004), based on similarities in geological and lithological make-up. This inference is further corroborated by the stratigraphic position as the greenstone belt underlies the Mesoproterozoic Chhattisgarh Supergroup (Das *et al.*, 2009; Parthanabis-Deb *et al.*, 2007). The Sonakhan granite-greenstone complex is a relatively small oblong belt with NNW-trending structural grain (Fig. 2). The lithostratigraphic succession of the Sonakhan belt was first worked out by Das *et al.* (1990). Later Saha *et al.* (2000) refined the lithostratigraphic succession of the greenstone which is given in Table 1. The Sonakhan Group comprises of (a) the lower Baghmara Formation consisting of dominantly metabasalt and subordinate felsic volcanics and (b) the upper Arjuni Formation consisting of greywacke and conglomerate.

Table 1. Stratigraphic succession of the Sonakhan Greenstone belt (Saha et al., 2000)

	Unit	Description	Intrusives
	Arjuni Formation	Thick succession of immature sandstone, polymict conglomerate, brown shale/ mudstone	Granophyre bodies and dioritic dykes
SONAKHAN	Unconformity		
GROUP	Baghmara Formation	Pillowed metabasalt, massive basalt with minor banded iron formation, greywacke, black shale and chert	Dykes or sills of felsic porphy or diorite

Figure 2. Geological map of the Sonakhan belt

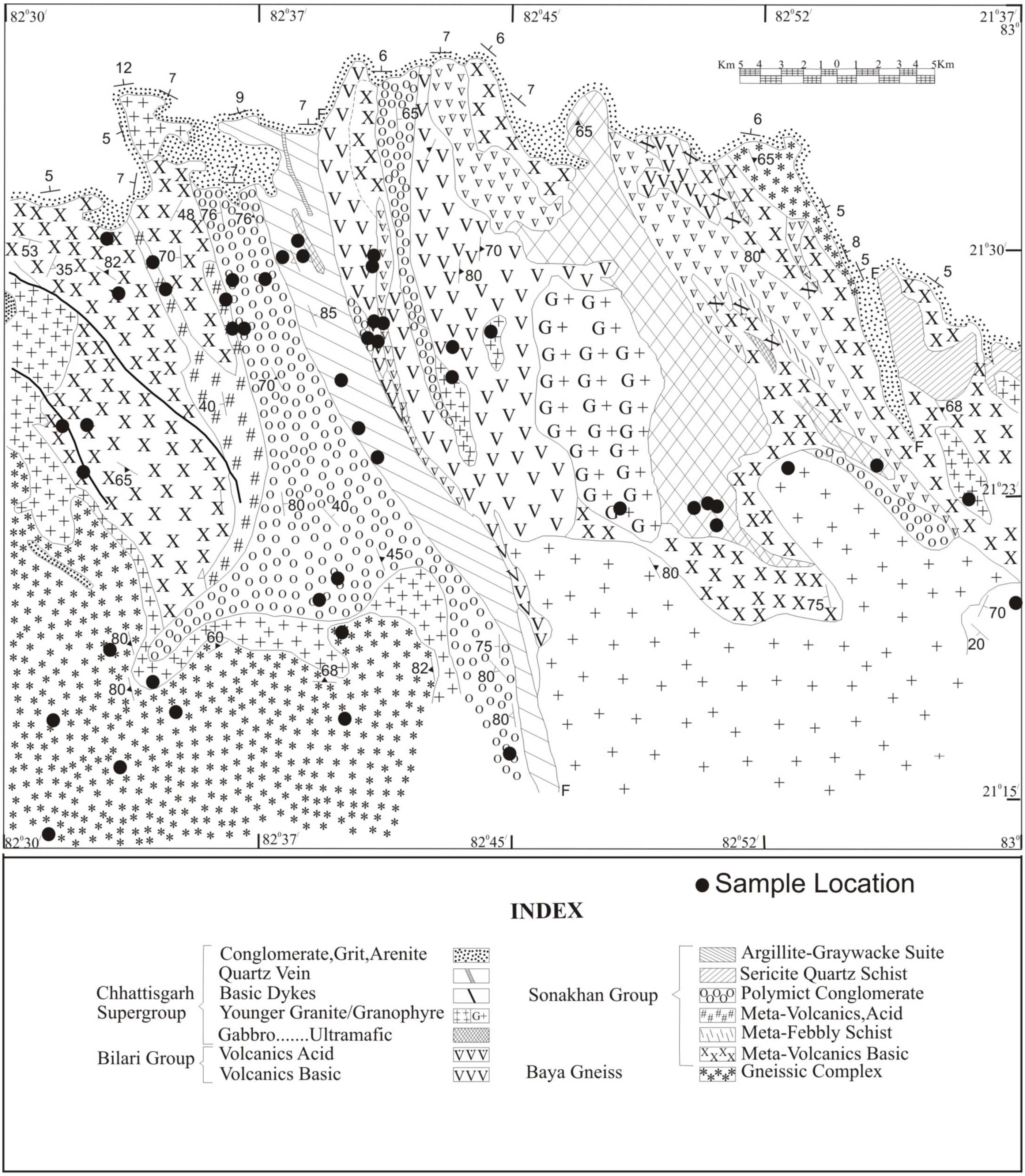

Geological map of the Sonakhan belt (Das *et al.*, 1990) showing important sample locations.

The suite of rocks belonging to the Baghmara Formation is dominated by massive through pillowed (Fig. 3), vesicular to amygdular basalt and constitute the lower unit of this formation, whereas the upper unit basalts are devoid of pillows. Minor rhyolite/felsic volcanics are associated with upper unit basalts. The Baya granitoids are intrusive into the Baghmara Formation (Fig. 4).

Figure 3. Baghmara Formation showing pillow structure

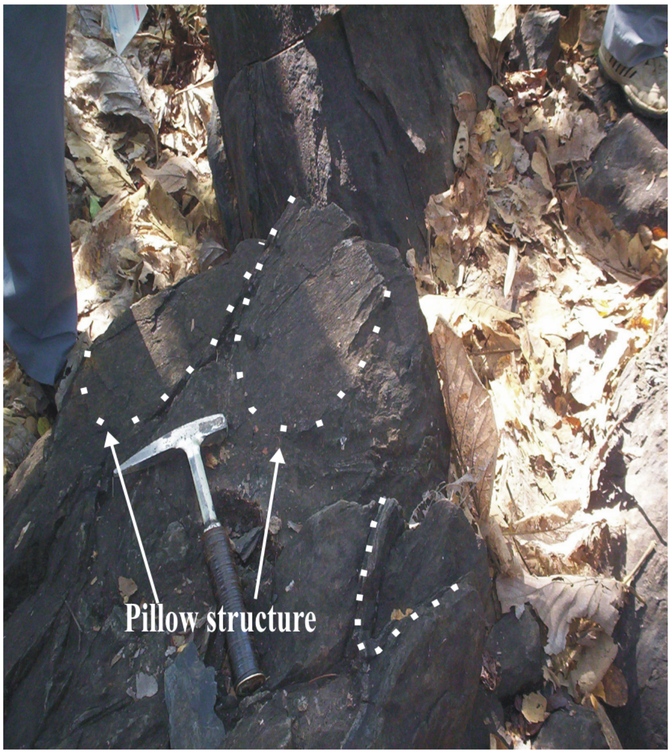

Field photograph of the lower unit basalts of the Baghmara Formation showing pillow structure near Jangla Pahar.

Figure 4. Schematic E-W cross section

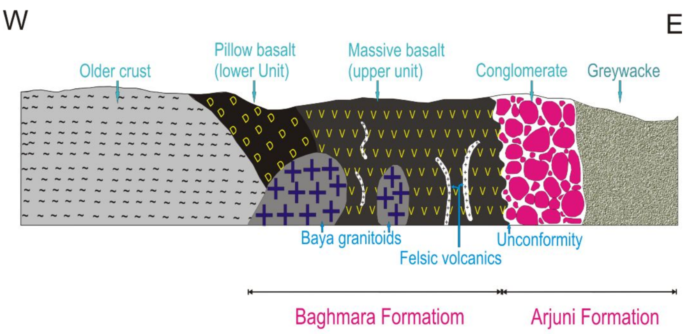

Schematic E-W cross section showing relationships among different litho-units of the Sonakhan Greenstone belt.

Field occurrence of the volcanic rocks

In the Sonakhan greenstone belt, a thick sequence of mafic volcanic rocks along with associated felsic variants constitutes the Baghmara Formation. The basaltic rocks are well exposed in the western part of the belt near Baghmara and Jangla Pahar. The lower part of the Baghmara Formation contains pillow basalts, referred to as, lower unit basalts. Individual pillows range in size from <10 cm to >40 cm in elongation. The overlying unpillowed massive basalts, referred to as, upper unit basalts, are well developed around Baya-Deopur-Deogarh hill road. Felsic rocks of rhyolitic composition and associated intermediate rocks occur as hillocks towards northwest of Runjhuni and west of Thelkadabri near Golajhar. They are generally greenish in colour and can be distinguished easily in the field. There is no unconformity between the two basaltic units.

Petrography

The Sonakhan Group of rocks as a whole has suffered greenschist facies of metamorphism but most of the basaltic rocks of the Baghmara Formation have well-preserved original igneous texture. These rocks are fine to medium grained, and in some cases, they exhibit porphyritic texture. In many basaltic samples primary pyroxenes have not reverted to chlorite and actinolite and the rock remains quite black. Since the rocks have overall preserved original igneous texture and mineralogy in most of the cases, we have retained the basalt term. The basaltic rocks mainly contain pyroxene, plagioclase and opaque minerals. The samples, which show effects of greenschist metamorphism, consist of chlorite, actinolite, plagioclase, epidote, sphene and opaque minerals. In some samples, biotite and hornblende have also been observed. The basaltic rocks exhibit limited alteration to chlorite, actinolite and epidote. Restricted alterations of plagioclase to sericite, and biotite and hornblende to chlorite, have been observed in many cases which may indicate in situ grain boundary controlled changes representing isochemical changes (Pollard *et al.*, 1983; Taylor and Pollard, 1988). Replacement of original pyroxene crystal by chlorite, and in some cases by amphiboles, without any change in original igneous texture, may also suggest isochemical changes (Redman and Kay, 1985).

Geochemistry

Sampling and Analytical Methods

Eighty one samples encompassing all the lithounits of the Baghmara Formation and the Arjuni Formation were collected as a part of a pilot project on tectonomagmatic evolution of the greenstone belts of the Bastar craton, central Indian shield. In this paper, we present the high precision geochemical data of the mafic and the felsic volcanic rocks of the Baghmara Formation. Samples were collected from exposures throughout the area based on accessibility, soil and forest cover. Utmost care was taken to collect fresh samples from unweathered exposures free from veins and amygdules. Locations of important sample collection sites are shown in Fig. 2. After careful petrographic evaluation for alteration, a total of 15 samples were selected for geochemical analysis. The selected samples include: 07 samples of Lower Unit basalt, 03 samples of Upper Unit Basalt and 05 samples of Felsic Volcanics (Table 2).

Table 2. Major (wt%) and trace element (ppm) data of the volcanic rocks of the Baghmara Formation of the Sonakhan Group

	Lower Unit Basalt								Upper Unit Basalts			Acid Volcanics				
Sample No.	S-709	S-710	S-711	S-712	S-713	S-714	P-733		S-758	S-762	S-763	J-717	J-718	J-719	A-736	A-737
SiO_2	49.44	50.24	51.94	49.98	47.67	50.22	48.93	SiO_2	51.72	69.39	57.8	69.96	70.02	65.73	53.25	58.94
TiO_2	1.07	0.83	0.97	1.05	1.27	1.16	1.07	TiO_2	0.79	0.56	0.61	0.34	0.33	0.31	1.17	1.74
Al_2O_3	12.81	13.77	11.79	13.86	13.17	13.48	13.36	Al_2O_3	14.94	15.92	13.9	15.86	15.37	17.28	16.31	19.44
$Fe_2O_3(T)$	14.23	12.73	12.86	13.74	16.15	13.82	14.84	$Fe_2O_3(T)$	6.93	3.18	7.52	3.18	3.17	3.97	15.92	8.84
MnO	0.19	0.18	0.21	0.2	0.2	0.21	0.18	MnO	0.11	0.02	0.1	0.01	0.03	0.03	0.18	0.07
MgO	7.11	7.74	7.39	6.84	7.98	7.06	7.59	MgO	3.61	1.19	6.62	0.66	0.8	0.82	6.51	1.9
CaO	11.84	12.12	11.68	10.31	10.59	10.56	11.14	CaO	8.87	1.17	5.18	0.58	2.26	1.81	0.61	0.64
K_2O	0.15	0.1	0.17	0.43	0.31	0.69	0.18	K_2O	1.27	5.05	2.51	3.39	3.22	3.51	0.74	1.21
Na_2O	1.92	2.03	2.39	3.22	1.63	2.87	1.86	Na_2O	3.22	1.25	3.38	3.69	3.47	3.52	1.07	1.88
P_2O_5	0.1	0.06	0.08	0.09	0.11	0.11	0.12	P_2O_5	0.11	0.19	0.21	0.09	0.1	0.08	0.05	0.1
LOI	2.04	1.08	1.79	1.67	1.56	1.04	1.87	LOI	8.82	2.89	3.01	3.78	3.01	2.78	5.78	4.42

	Lower Unit Basalt								**Upper Unit Basalts**			**Acid Volcanics**				
Total	100.89	100.88	101.27	101.41	100.65	101.23	101.14	*Total*	100.39	100.82	100.84	101.54	101.77	99.85	101.59	99.19
Cu	103	92	49	121	203	64	61	Cu	53	10	35	0	0	0	2	2
Zn	68	46	63	79	66	80	65	Zn	40	35	56	16	16	15	23	22
Pb	13	146	12	13	69	67	11	Pb	161	74	24	50	127	65	114	49
Ga	15	14	11	17	16	15	16	Ga	15	21	18	22	23	23	17	21
Cr	283	391	272	471	170	144	296	Cr	211	42	326	3	2	2	24	16
Co	60	55	66	113	74	55	63	Co	34	7	32	11	12	11	64	42
Ni	109	151	135	171	101	97	138	Ni	95	14	104	2	1	1	10	6
Rb	3	3	4	13	11	12	4	Rb	37	240	84	105	96	107	20	35
Sr	102	118	156	156	139	140	122	Sr	413	74	527	272	343	383	69	85
Cs	0.25	0.41	0.09	0.31	0.28	0.27	0.14	Cs	3.11	4.73	1.33	4.39	3.16	4.41	0.52	0.69
Ba	108	185	139	166	143	299	131	Ba	531	1093	867	921	844	1044	289	302
Sc	43	46	41	44	45	39	38	Sc	25	11	15	3	4	3	30	23
V	291	281	283	309	316	271	292	V	143	37	114	14	15	16	114	128
Ta	0.26	0.32	0.46	0.43	0.47	0.17	0.34	Ta	0.27	1.29	0.6	0.89	0.89	0.62	0.33	0.51
Nb	3	2	3	3	4	3	4	Nb	3	22	9	6	6	6	2	3
Zr	11	20	10	35	37	23	16	Zr	106	364	192	95	104	99	23	52
Hf	1	1	1	1	1	1	1	Hf	3	9	4	3	3	3	1	2
Th	0.18	0.16	0.27	0.33	0.2	0.3	0.43	Th	4	26	8	12	12	11	0.47	0.63
U	0.07	0.05	0.1	0.1	0.36	0.09	0.1	U	1	6	2	2	2	9	0.26	0.35
Y	26	21	24	24	28	26	28	Y	14	47	18	10	10	10	9	13
La	3.4	2.5	3.6	4.4	4.1	4.6	4.4	La	23.2	88.9	47.1	47.5	48.4	37.7	2.8	7.3
Ce	8.5	6	8.5	9.9	9.3	10.6	10.3	Ce	39.9	144.3	79.6	85	86.4	67.5	6.7	14.6

	Lower Unit Basalt								Upper Unit Basalts			Acid Volcanics				
Pr	1.3	0.9	1.3	1.4	1.5	1.5	1.5	Pr	4.4	14.8	8.5	8.6	8.7	6.8	1	2.3
Nd	8	5.6	7.4	8.5	9	9	8.9	Nd	19.7	61.7	37.3	30.8	31.2	24.7	4.9	11.4
Sm	2.5	1.9	2.3	2.6	2.9	2.7	2.9	Sm	3.7	10.9	6.3	4.4	4.5	3.6	1.4	2.8
Eu	0.9	0.7	0.7	1	1	1	1	Eu	1.1	2.1	1.7	1.2	1.1	1	0.5	0.7
Gd	3	2.2	2.8	2.9	3.3	3.1	3.2	Gd	3.2	10	5.4	3.4	3.5	2.9	1.2	2.1
Tb	0.5	0.4	0.5	0.5	0.6	0.5	0.6	Tb	0.4	1.3	0.6	0.4	0.4	0.3	0.2	0.3
Dy	3.9	3.1	3.6	3.6	4.3	3.9	4.2	Dy	2.2	7.6	3.1	1.9	1.9	1.7	1.7	2.3
Ho	0.9	0.7	0.8	0.8	0.9	0.9	0.9	Ho	0.5	1.5	0.6	0.2	0.2	0.2	0.2	0.3
Er	2.3	1.8	2.1	2.1	2.5	2.3	2.5	Er	1.2	3.9	1.5	0.6	0.6	0.6	0.6	0.9
Tm	0.3	0.2	0.3	0.3	0.3	0.3	0.3	Tm	0.2	0.5	0.2	0.1	0.1	0.1	0.1	0.1
Yb	1.7	1.4	1.5	1.5	1.8	1.7	1.8	Yb	0.9	2.6	1	0.6	0.7	0.7	1	1.4
Lu	0.4	0.3	0.3	0.3	0.4	0.4	0.4	Lu	0.2	0.6	0.2	0.1	0.1	0.1	0.2	0.2
$(Nb/Th)_{pm}$	2	1.6	1.5	1.1	2.2	1.2	1	$(Nb/Th)_{pm}$	0.1	0.1	0.1	0.1	0.1	0.1	0.5	0.6
$(La/Th)_{pm}$	2.3	1.9	1.7	1.6	2.5	1.9	1.3	$(La/Th)_{pm}$	0.8	0.4	0.7	0.5	0.5	0.4	0.7	1.4
$La/Nb)_{pm}$	1.1	1.2	1.1	1.4	1.1	1.5	1.3	$La/Nb)_{pm}$	9.5	4.2	5.7	7.7	7.9	6.5	1.4	2.4
$(La/Yb)_{cn}$	1.5	1.4	1.7	2.1	1.6	1.9	1.7	$(La/Yb)_{cn}$	18.4	24.3	35.3	54.5	50.4	39.1	2	3.6

	Lower Unit Basalt								**Upper Unit Basalts**			**Acid Volcanics**				
$(La/Sm)_{cn}$	0.9	0.8	1	1.1	0.9	1.1	1	$(La/Sm)_{cn}$	4.1	5.3	4.8	7	6.9	6.8	1.3	1.7
$(Gd/Yb)_{cn}$	1.5	1.3	1.5	1.6	1.5	1.5	1.5	$(Gd/Yb)_{cn}$	2.9	3.2	4.7	4.5	4.2	3.4	1	1.2
Nb/Yb	1.9	1.6	2.1	2.1	2.1	1.8	1.9	Nb/Yb	2.8	8.3	9	10.3	9.2	8.8	2.1	2.2
Ta/Yb	0.2	0.2	0.3	0.3	0.3	0.1	0.2	Ta/Yb	0.3	0.5	0.6	1.4	1.3	0.9	0.3	0.4
Nb/Ta	11.8	6.6	7.2	7.4	7.9	18.6	10.5	Nb/Ta	9.5	16.9	14.4	7.2	7.2	9.7	6.5	6.1
Y/Ho	30.7	31.2	30.2	31.1	29.9	30.3	29.5	Y/Ho	28.8	31	31.8	53.8	53.1	54	46	48
Zr/Y	0.4	1	0.4	1.4	1.3	0.9	0.6	Zr/Y	7.9	7.8	10.5	9.6	10.5	10.4	2.6	4
Ti/Zr	5597	2331	5276	1688	1925	2848	3700	Ti/Zr	415	85	178	202	177	173	2858	1889
Nb/Y	0.1	0.1	0.1	0.1	0.1	0.1	0.1	Nb/Y	0.2	0.5	0.5	0.6	0.6	0.6	0.2	0.2
$(Zr/Sm)_{pm}$	0.2	0.4	0.2	0.5	0.5	0.3	0.2	$(Zr/Sm)_{pm}$	1.2	1.3	1.2	0.9	0.9	1.1	0.7	0.7
$(Ti/Sm)_{pm}$	0.9	0.9	0.9	0.8	0.9	0.9	0.8	$(Ti/Sm)_{pm}$	0.4	0.1	0.2	0.2	0.1	0.2	1.7	1.3

	Lower Unit Basalt								Upper Unit Basalts			Acid Volcanics				
(Eu/Eu*)	1	1.1	0.8	1.1	1	1	1	(Eu/Eu*)	1	0.6	0.9	0.9	0.9	1	1.1	0.9
Nb/Nb*	1.4	1.2	1.2	1	1.5	1	0.9	Nb/Nb*	0.1	0.2	0.2	0.1	0.1	0.1	0.7	0.5
Zr/Hf	15.3	28.3	17.3	30.4	25.8	23.2	20.8	Zr/Hf	41.1	41.8	43.4	33.1	33.6	32	31.1	34.4
$(Nb/La)_{pm}$	0.9	0.8	0.9	0.7	0.9	0.6	0.8	$(Nb/La)_{pm}$	0.1	0.2	0.2	0.1	0.1	0.2	0.7	0.4
Nb/Y	0.1	0.1	0.1	0.1	0.1	0.1	0.1	Nb/Y	0.2	0.5	0.5	0.6	0.6	0.6	0.2	0.2
Nb/U	46.4	42.9	34.6	32.8	10.3	34.3	34.8	Nb/U	2.5	3.3	3.8	3	2.8	0.7	8.5	8.8
Nb/Th	17.1	13.2	12.4	9.6	18.6	10.4	8.3	Nb/Th	0.7	0.8	1.1	0.5	0.5	0.6	4.6	5
Nb/La	0.9	0.8	0.9	0.7	0.9	0.7	0.8	Nb/La	0.1	0.2	0.2	0.1	0.1	0.2	0.8	0.4

Approximately 1 kg of each rock sample was crushed to ~2 mm size chips and about 50 g split of each sample was pulverized to -200 mesh fine powder in an agate mill. Major elements were analyzed by SIEMENS SRS 3000 sequential X-Ray Fluorescence (XRF) Spectrometer on fused discs glued with polyvinyl alcohol at the Wadia Institute of Himalayan Geology, Dehra Dun, whereas trace elements, including rare earth elements, were analyzed at the National Geophysical Research Institute, Hyderabad by inductively coupled plasma mass spectrometer (ICP-MS, Perkin Elmer SCIEXELAN DRC II). The samples were fused with $LiBO_2$ followed by treatment with HNO_3 and further dilution of dissolved bead solution to 250 ml to reduce the total dissolved solids to less than 0.12% in fluid solution as proposed by Roy *et al.* (2007). The analytical accuracy of the major oxide data is <5% and the average precision is always better than 1.5 %. The precisions achieved for ICP-MS analyses were <5% RSD with comparable levels of accuracy. International standards were used for calibration and testing of accuracy. The geochemical data are presented in Table 2.

Assessment of alteration and element mobility

Only those samples were selected for geochemical analysis, which show the least alterations. Important chemical modifications that generally take place in subaqueous spilitization process, deuteric alteration and greenschist facies metamorphism include: high loss on ignition (LOI) values, scatter and inconsistency of major element data. The studied samples have low LOI (mostly < 3 wt%), except for a few which show slightly high LOI values. In addition to low LOI for the most of the samples, the most of the major elements and trace elements including large ion lithophile elements (LILE), high field strength elements (HFSE) and rare earth elements (REE) exhibit coherent intra- and inter-sample behaviour of the samples. However, the significant variations in some major elements, notably $Na2_O$, K_2O, SiO_2 and LOI may be due to alteration. There are no erratic or spurious anomalies in the REE patterns of the samples. These observations suggest that elemental variations in the samples reflect primary igneous processes. Nevertheless, our petrogenic interpretations of the rocks heavily rely on immobile trace elements.

Major and trace element variations

Lower Unit Basalts

The basalts from the lower part of the Baghmara Formation plot in the subalkaline basalt field (Fig. 5) on the immobile trace elements based discrimination diagram of Winchester and Floyd (1977). They are characterized by 47.67 to 51.94 wt% SiO_2, 6.84 to 7.98 wt% MgO, 12.73 to 16.15 wt% Fe_2O_3(T), 11.79 to 13.86 wt% Al_2O_3, 0.83 to 1.27 wt% TiO_2 and 10.31 to 12.12 wt% CaO (Fig. 6, Table 2). They have lower concentrations of Ni (97- 171 ppm, mean 129 ppm) and Cr (144-471 ppm, mean 289 ppm) (Fig. 7, Table 2) compared to N-MORB (Hofmann, 2004). These values are too low for magmas that have equilibrated with peridotite mantle (Roeder and Emsile, 1970). Thus, the lower unit basalts appear to have undergone fractionation. They possess sub-chondritic Nb/Ta values (6.62 – 18.62) except for one sample (S-714) which has super-chondritic Nb/Ta value of 18.62 (chondritic values after Sun and McDonough, 1989). Ti/Zr ratios of these samples are consistently higher (1687-5597) than the chondritic value (111.98). The ratios of Zr/Y and Zr/Hf range from 0.41 to 1.45 and 15.34 to 30.43, respectively which are less than those of chondrite (2.46 and 36 respectively). On the chondrite-normalized diagram (Sun and McDonough, 1989) (Fig. 8), the lower unit basalts exhibit near-flat REE pattern. On the primordial mantle-normalized multi-element diagram (Sun and McDonough, 1989) (Fig. 9), the samples show N-MORB like La-Nb-Th patterns having ratios of $(La/Nb)_{pm}$ = 1.14 – 1.56; $(La/Th)_{pm}$ = 1.28 – 2.54; $(Nb/Th)_{pm}$ = 0.99- 2.22). They also show depletion of Ti relative to middle rare earth elements (MREE) having ratios of $(Ti/Sm)_{pm}$ = 0.77 – 0.89). Some important trace element characteristic features of the lower unit basalts are their Nb-anomalies which are either zero-anomalies or positive-anomalies (Nb/Nb* = 0.93 – 1.48). All these geochemical features along with pillow structures are consistent with oceanic plateau basalts which are generated by a rising mantle plume (Sandeman *et al.*, 2006; Van Boening and Nabelek, 2008).

Figure 5. Nb/Y vs. Zr/Ti classification diagram

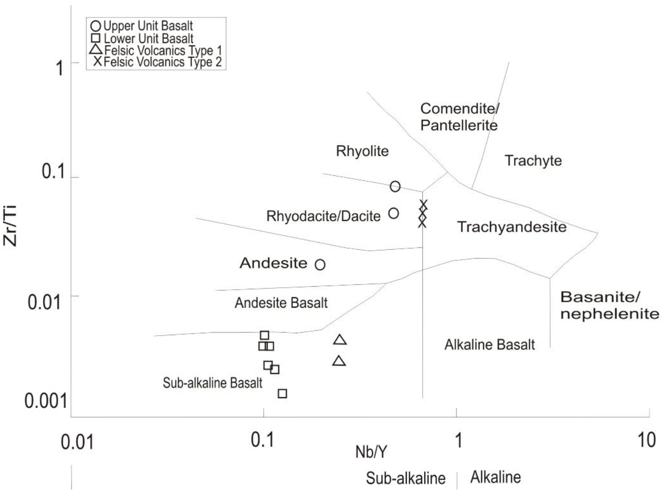

Nb/Y vs. Zr/Ti classification diagram (Winchester and Floyd, 1977) of the volcanic rocks of the Baghmara Formation.

Figure 6. SiO_2 vs. TiO_2, Fe_2O_3(T), Al_2O_3, MgO and CaO variation diagram

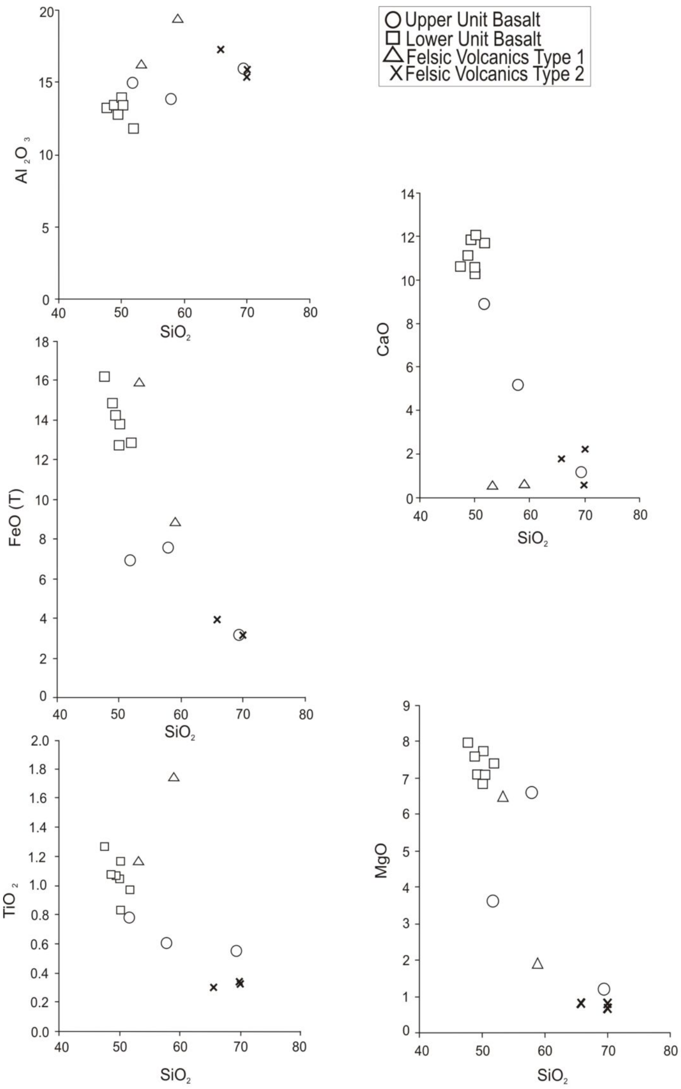

SiO_2 vs. TiO_2, Fe_2O_3(T), Al_2O_3, MgO and CaO variation diagram of different litho-units of the Sonakhan Greenstone belt.

Figure 7. SiO_2 vs. V, Rb, Ni, Y, Sr, Co, Zr, Th and Cr variation diagram

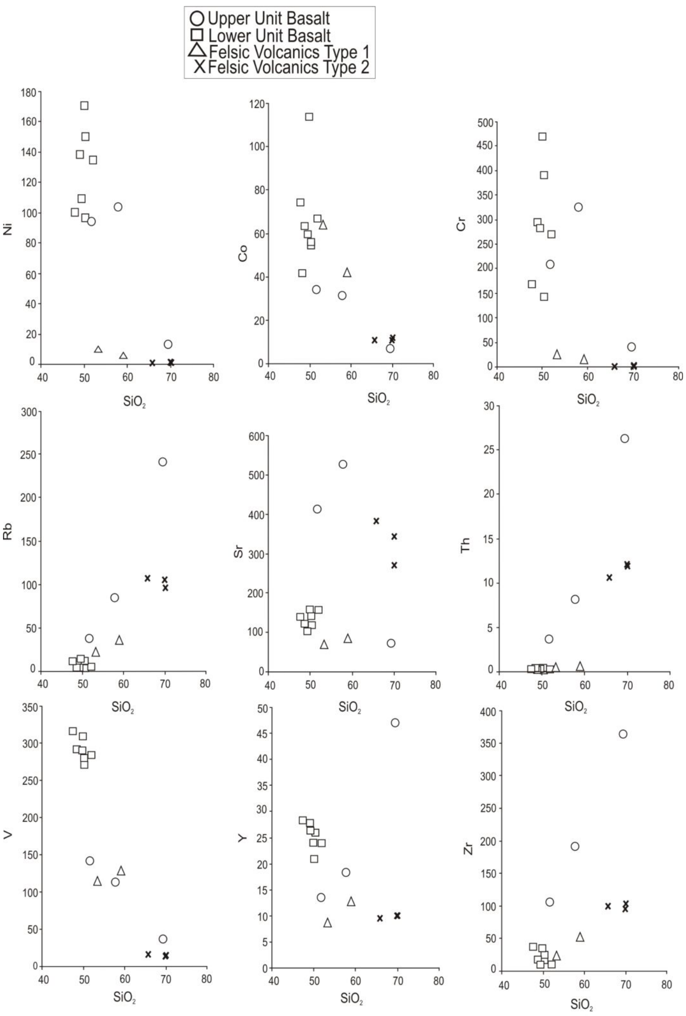

SiO_2 vs. V, Rb, Ni, Y, Sr, Co, Zr, Th and Cr variation diagram of different litho-units of the Sonakhan Greenstone belt.

Figure 8. Chondrite-normalized REE patterns

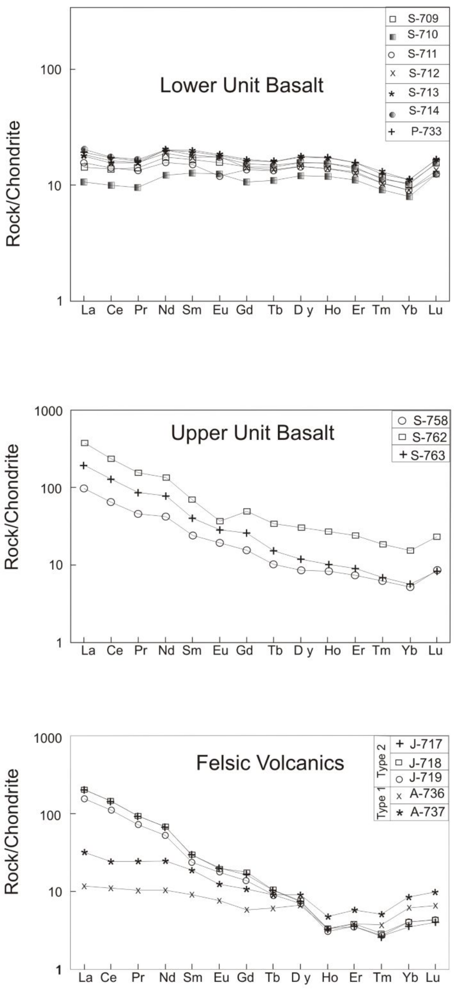

Chondrite-normalized (Sun and McDonough, 1989) REE patterns of the volcanic rocks of the Baghmara Formation.

Figure 9. Primordial mantle-normalized multi-element patterns

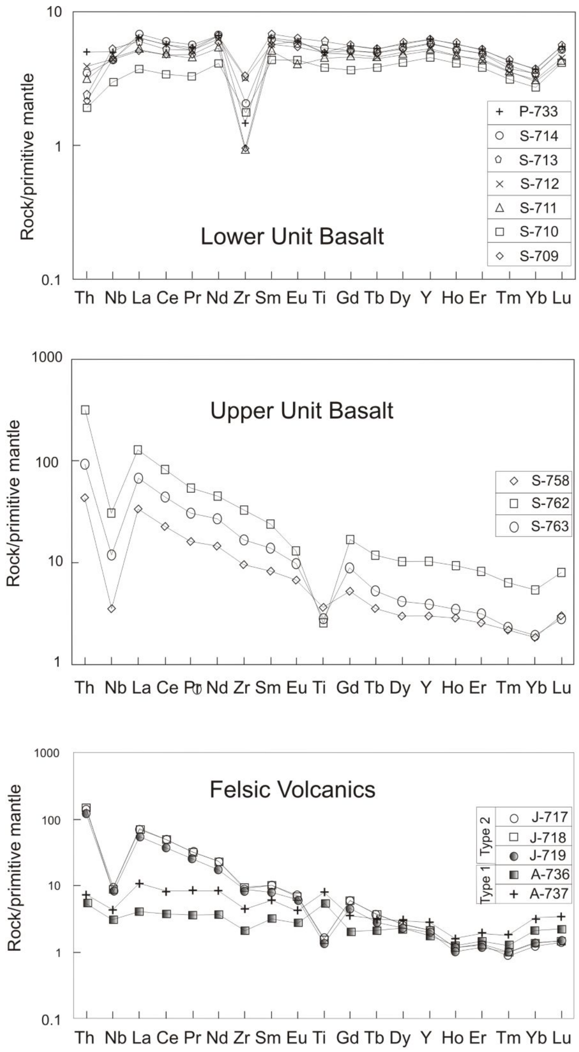

Primordial mantle-normalized (Sun and McDonough, 1989) multi-element patterns of the volcanic rocks of the Baghmara Formation.

Upper Unit Basalts

The upper unit basalts of the Baghmara Formation of the Sonakhan Group are subalkaline basalts ranging in composition from andesite through dacite to rhyolite (Fig. 5). These basalts are characterized by 51.72 – 69.39 % SiO_2, 0.56 – 0.79% TiO_2, 1.19 – 6.62% MgO, 13.90 – 15.92% Al_2O_3 and 3.18 – 7.52% Fe_2O_3(T) (Table 2, Fig. 6). There are large variations in Ni (13 - 104 ppm), Cr (42-326), V (37- 143 ppm), Zr (106- 364 ppm), Co (13 – 104 ppm) and Y (13 – 47 ppm) (Table 2, Fig. 7). The ratios of Ti/Zr (85 – 414) are sub- to super-chondritic, whereas Zr/Y ratios (8- 10) are always super-cohondritic.

In addition, they have the following trace element characteristics: highly fractionated REE patterns having $(La/Yb)_{cn}$ = 18.39 to 35.27, $(La/Sm)_{cn}$ = 4.1 – 5.29, $(Gd/Yb)_{cn}$ = 2.89 – 4.66); minor negative to no Eu-anomalies (Eu/Eu* = 0.62 – 1.02) and large negative Nb-anomalies [$(Nb/Th)_{pm}$ = 0.08 – 0.13; $(Nb/La)_{pm}$ = 0.10 – 0.24] (Fig. 5 & 6, Table 2). Nb/Nb* of these basalts are always very low (Nb/Nb* <0.16). These features are closely similar to those of subduction related island arc basalts (Polat et al, 2005; Polat and Hofmann, 2003). Since the upper unit basalts are enriched in LILE and LREE, and depleted in HFSE, particularly in Nb, Ta and Ti on the normalized trace element diagrams, it is proposed that they represent typical island arc lavas.

Felsic Volcanic Rocks

The felsic volcanic rocks of the Baghmara Formation of the Sonakhan Group are characterized by 53.25 – 70.02% SiO_2, 0.31 – 1.74% TiO_2, 0.66 – 6.51% MgO, 15.37 – 19.44% Al_2O_3, 3.17 – 15.92% $Fe_2O_3(T)$ (Table 2, Fig. 6). Compared to the upper unit basalts, these felsic volcanics are depleted in Ni (1 - 10 ppm), Cr (2-24 ppm) and Zr (23- 104 ppm) but comparable in V contents (14- 128 ppm) (Table 2, Fig. 7). The ratios of Ti/Zr (85 – 414) are sub- to super-chondritic, whereas Zr/Y ratios (8- 10) are always super-cohondritic. In addition, they have the following trace element characteristics: moderately to highly fractionated REE patterns having $(La/Yb)_{cn}$ = 1.97 to 54.55, $(La/Sm)_{cn}$ = 4.1 – 5.29, $(Gd/Yb)_{cn}$ = 2.89 – 4.66; minor negative Eu-anomalies (Eu/Eu* = 0.62 – 1.02) and large negative Nb anomalies [$(Nb/Th)_{pm}$ = 0.08 – 0.13; $(Nb/La)_{pm}$ = 0.10 – 0.24] (Fig. 8 & 9, Table 2). Like the upper unit basalts, the felsic volcanics also exhibit low values of Nb/Nb* (0.10 – 0.68). The felsic volcanics can be divided into two types based on multi-element patterns (Fig. 9): Type 1: samples with minor negative Nb-anomaly but positive Ti-anomaly and Type 2: samples with pronounced negative Nb- and Ti-anomalies. The patterns of type 1 rocks may be a fractionated product of plume-generated basaltic rocks, very much similar to those of the lower unit basalt. Multi-element patterns of the type 2 felsic rocks are fractionated and are very much similar to those of the upper unit basalt of island arc affinity.

Petrogenetic evidence

Contamination of the basalts of the Baghmara Formation of the Sonakhan greenstone belt by continental crust during the magma ascent may be ruled out on the basis of their geochemical characteristics and the presence of the pillowed structure which is consistent with an oceanic, rather than a continental setting. There is also no field evidence to indicate that the Sonakhan greenstone basalts were emplaced in an older continental basement.

The REE patterns of the lower unit basalts of the Baghmara Formation of the Sonakhan greenstone belt are near-flat (slightly LREE-depleted to slightly LREE-enriched) (Fig. 8) and the rock types are subalkaline in composition (Fig. 5). These rocks have positive (to slightly negative) Nb-anomalies (Nb/Nb* = 0.93 – 1.48, mean 1.17, Table 2). All of these features are consistent with an oceanic plateau association generated by a mantle plume. The near-flat REE patterns may have resulted from the high degrees of partial melting in the mantle plume. Nb/Y ratio of the lower unit basalts ranging from 0.10 to 0.14 at the SiO_2 level of 47.67 to 51.94%, indicates that the basalts were generated from the high percentage of melting at shallow depth (Greenough *et al.*, 2005). The REE and incompatible multi-element patterns of these basalts are similar to those of many modern, Proterozoic and Neoarchaean ocean islands (Polat, 2009 and references therein). The multi-element patterns of the lower unit also exhibit distinct negative Zr-anomalies (Fig. 9). Their Nb/U ratio ranges from 10.27 to 46.39 which is chondritic to super-chondritic (Nb/U = 31 in chondrite). Similarly the La/U (11.36 – 51.26) and Nb/Th ratios (8.29- 18.59) are also chondritic to super-chondritic (La/U and Nb/Th values in chondrite are 30, 8.5 respectively). The Nb/La ratios (0.67 – 0.91) are sub-chondritic to chondritic (chondrite value is 1.0). These features are considered to be typical of ocean island basalt. Based on the geochemical and the field characteristics, it is proposed that the lower unit basalts of the Baghmara Formation represent an oceanic plateau erupted from a rising mantle plume. Type 1 felsic volcanic rocks with minor negative Nb-anomaly and positive Ti- anomaly may represent differentiated product of plume generated basaltic rock.

The upper unit basalts and the associated type 2 felsic volcanic rocks show chemical characteristics of the island arc volcanic association having larger variations in major and trace elements, ranging from sub-alkaline basalt through andesite, dacite to rhyolite (Fig. 5) forming a BADR (basalt-andesite-dacite-rhyolite) series. Similar patterns have recently been reported from the arc-related Gadwal greenstone belt of the Dharwar craton (Manikyamba and Khanna, 2007). Our samples of the upper unit basalts have distinct Th-Nb-REE systematics. The upper unit basaltic rocks and the type 2 felsic rocks are characterized by the positively fractionated REE patterns (Fig. 8). They also display strong depletion in Nb and Ti relative to Th, LREE and MREE (Fig. 9). Nb/U (2.46-3.77), Nb/Th (0.68 – 1.5) and Nb/La (0.11 – 0.24) ratios are sub-chondritic. They have higher Zr/Y ratios (7.76-10.51) compared to those of the lower unit basalt (0.41- 1.45) of the oceanic plateau association. The REE and the trace element patterns shown by the upper unit basalts and the associated type 2 felsic volcanics are very much similar to those of the volcanic rocks of the island arc setting. Such patterns have been reported from several Arcahean greenstone belts (Hollings and Kerrich, 2000; Wyman *et al.*, 2000; Hollings, 2002; Sanderman *et al.*, 2004).

Tectonic setting

Pearce (2008) has suggested that the E-MORB and OIB sources are enriched relative to N-MORB sources that are revealed by the high Ta/Yb and Th/Yb ratios yielding a MORB-OIB array (Fig. 10). Crust input, either by magma-crust interactions or by crustal recycling into magma sources, raises the Th/Yb ratios that plot above this MORB-OIB array. On the Ta/Yb vs Th/Yb diagram (Fig. 10), the lower unit basalts plot close to E-MORB within the array. On the other hand, the upper unit basalts and the felsic volcanics (except for the two felsic volcanic samples which plot close to E-MORB) plot mainly within the volcanic arc field.

Figure 10. Ta/Yb vs. Th/Yb diagram

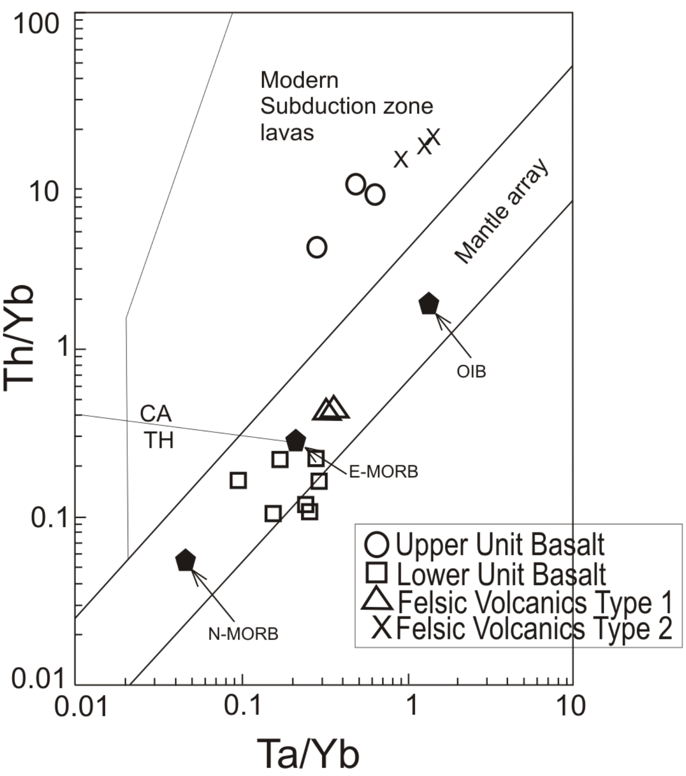

Ta/Yb vs. Th/Yb diagram for the volcanic rocks of the Baghmara Formation. Data for N-MORB, E-MORB, OIB are after Sun and McDonough (1989). Fields after Pearce (1982, 2003). CA, Calc-alkaline; TH, tholeiite.

It is proposed that the Sonakhan greenstone belt contains rocks of both the oceanic plateau association and the island arc association. It is noteworthy that the lower unit pillowed oceanic plateau basalt and the upper unit basalt of the island arc association are not spatially related with unconformity in between them, although both the rock types were emplaced in different tectonic settings. The lower unit pillowed basalt and the upper unit basalt along with felsic volcanics occur even without any obvious structural discontinuity. This indicates that the relationship between these two lithotypes is primary and may indicate tectonic juxtaposition of the island arc association over the oceanic plateau association. This, in turn, may indicate co-existence of contemporaneous plume and arc magmatism in the Sonakhan greenstone belt. The plume derived plateau basalts occupy the lower part of the Baghmara Formation and predate the upper unit calc-alkaline basalt, andesite, dacite and rhyolite series of the Baghmara Formation of the island arc association. Thus, the Bhagmara Formation, as a whole, represents both plume type and island arc type volcanism (Fig. 11).

Figure 11. Geodynamic evolution of the Sonakhan Greenstone belt

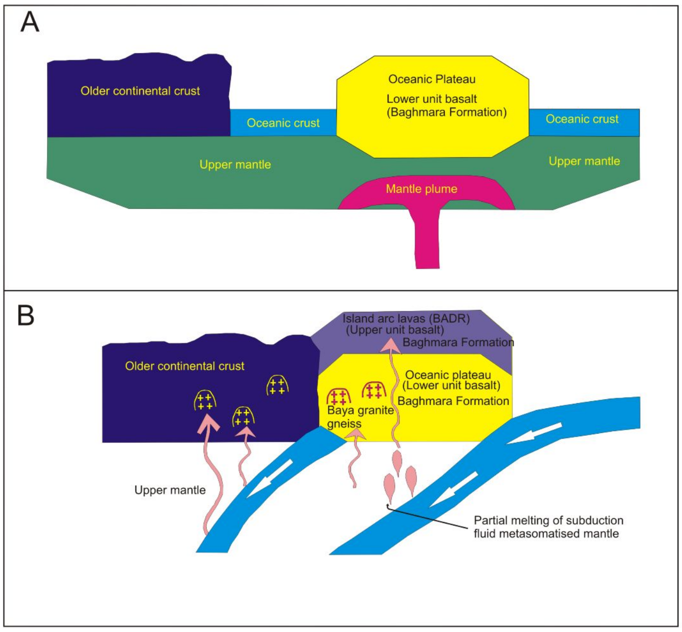

Cartoon showing the geodynamic evolution of the Sonakhan Greenstone belt. A. Eruption of the plume-related basalt forming the oceanic plateau (lower unit basalt of the Baghmara Formation). B. Subduction of the oceanic plate under the oceanic plateau resulting in arc-related magma.

The operation of the subduction process in this part of the Indian shield is also indicated by geochemical characteristics of the Baya gneisses (Hussain *et al.*, 2004; Mondal *et al.*, 2006). It appears that partial melting of the mantle wedge which was metasomatized by slab released – fluids has given rise to rocks of the basalt-andesite-dacite-rhyolite association of the upper unit basalt of the Baghmara Formation. Lithospheric extension in the overriding plate may have occurred in response to subduction slab-rollback resulting in the formation of an intra-arc basin where the clastics of the Arjuni Formation were deposited. In the absence of geochronological data, the timing of these processes remains speculative. However, based on the lithological make-up and the stratigraphic positions, a broad age band of Neoarchaean to Paleoproterozoic may be assigned to the Sonakhan greenstone belt. Hollings and Kerrich (2006) reported the presence of such compositionally diverse, spatially associated basaltic flows in the 2.7 Ga St. Joseph greenstone belt, Canada.

Evolutionary Model

The geochemical data-derived interpretations in combination with the overall lithological make-up of the Sonakhan granite-greenstone belt can be used to suggest a model for the tectonomagmatic evolution of the Bastar craton of the Indian shield. It is proposed that during late Archaean, a rising mantle plume generated a thickened, hot, buoyant and so unsubductable oceanic plateau, that is now represented by the lower unit basalts of the Baghmara Formation. The accretion of this plateau against an old continent margin could have triggered subduction. The thick oceanic plateau served as a base for further subduction of the oceanic crust producing subduction-related basaltic and felsic volcanic rocks, consisting of upper unit basalts, in an island arc setting (Fig. 11). The magmas might have been derived from the fluid-metasomatized mantle wedge producing the upper unit basalts of the island arc affinity. A similar model has been proposed for the evolution of the Western Dharwar Craton by Naqvi *et al.* (2006); Manikyamba and Khanna (2007) and Jayananda *et al.* (2008). In response to subduction slab roll-back, lithospheric extension in the over-riding plate may have occurred causing rifting of the arc. This extension may have eventually led to the formation of an intra-arc basin in which clastics of the Arjuni Formation were deposited. Petrographical and geochemical characteristics of these clastic rocks also corroborate this contention (our preliminary unpublished data). The plume-arc interaction model proposed here for the Sonakhan greenstone belt may be applicable for the Bastar craton as a whole during the Neoarchaean to Paleoproterozoic. Since such model has also been proposed for the Dharwar craton, it may further point to the dominance of such process for the evolution of the Indian shield during the Neoarchaean to Paleoproterozoic.

Conclusions

The field and the geochemical data suggest the presence of two volcanic rock associations in the Sonakhan greenstone belt: (1) an oceanic plateau association composed dominantly of tholeiite basalts and (2) a compositionally diverse intra-oceanic island arc association. The latter association is composed of tholeiite to andesite, dacite and rhyolite (BADR series). The REE patterns of the Sonakhan greenstone oceanic plateau basalts vary from depleted N-MORB like, to flat oceanic plateau like. Similar REE patterns have been reported from the

Phanerozoic plume-derived oceanic plateaus and ocean islands (Kerr and Mahoney, 2007; Kerr, 2004; Hofmann, 2004). The presence of both the oceanic plateau and the island arc association in the Sonakhan greenstone belt can be explained by the initiation of a subduction zone at the edge of an oceanic plateau. Compositionally diverse lavas including basalts, andesite, dacite, rhyolite erupted from an island arc developed at the edge of the oceanic plateau. Extension of the overriding plate led to the rifting of the arc, resulting in the formation of an intra-arc basin for the deposition of the clastic rocks now represented by the Arjuni Formation. Thus, it is apparent that the plume-arc interaction model is a viable mechanism for the evolution of the continental crust during the Neoarchaean to Paleoproterozoic.

Acknowledgements

The authors are thankful to the Chairman, Department of Geology, AMU, Aligarh for providing the facilities. Dr. V. Balaram, National Geophysical Research Laboratory, Hyderabad and Dr. N. K. Saini, Wadia Institute of Himalayan Geology, Dehra Dun are thanked for providing analytical facilities. Financial assistance by the DST, Govt. of India to carry out this work (SR/S4/ES-180/2005) is duly acknowledged. We express our sincere thanks to Prof. Talat Ahmad for inviting us to contribute to this special volume. We are grateful to Prof. D.K. Paul, Prof. Rajesh K. Srivastava and Dr. Vivek K. Malviya for constructive and helpful reviews and suggestions that led to considerable improvements in the final version of the manuscript.

References

Abbott, D.H., Drury, R. and Mooney, W.D., 1997. Continents as lithological icebergs: the importance of buoyant lithospheric roots. Earth Planet. Sci. Lett., 149 : 15-27. 10.1016/S0012-821X(97)00065-4

Crookshank, H., 1963. Geology of southern Bastar and Jeypore from Bailadila range to eastern ghats. Geol. Surv. India, Mem. 87, 96 - 108.

Das, K., Yokoyama, K., Chakraborty, P.P. and Sarkar, A., 2009. Basal tuffs and contemporaneity of the Chattisgarh and Khariar basins based on new dates and geochemistry. Jour. Geology, 117, 88-102.

Das, N., Royburman, K.J, Vasta, U.S and Mahurkar, Y.V, 1990. Sonakhan schist belt - a Precambrian granite-greenstone complex. GSI Spl. Pub. No. 28, 118-132.

Desrochers, J., Hubert, C., Ludden, J.N. and Pilote, P., 1993. Accretion of Archaean oceanic fragments in the Abitibi greenstone belt, Canada. Geology, 21: 451-454. 10.1130/0091-7613(1993)021<0451:AOAOPF>2.3.CO;2

Dostal, J. and Muller, W.U, 2004. Komatiite geochemistry. In: Eriksson, P.G., Altermann, W., Nelson, D.R., Muller, W.U, Catuneanu (Eds.), The Precambrian Earth: Tempos and events, elsevier, Amsterdam, pp. 290-298.

Dostal, J., Muller, W.U. and Murphy, J.B., 2004. Archaean molasses basin evolution and magmatism, Wabigoon Subprovince, Canada. J. Geol., 112: 435-454. 10.1086/421073

Galer, S.J.G. and Mezger, K., 1998. Metamorphism, denudation and sea level in the Archaean and cooling of the earth. Precam. Res., 92: 389-412. 10.1016/S0301-9268(98)00083-7

Greenough, J.D., Dostal, J. and Mallory-Greenough, L.M., 2005. Oceanic island volcanism II: mantle processes. Geosci. Can., 38: 23-40.

Hofmann, A.W., 2004. Sampling mantle heterogeneity through oceanic basalts : Isotopes and trace elements. In : Carlson, R.W. (Ed.), Treatise on Geochemistry, Vol. 2, pp. 61-101.

Hollings, P. and Kerrich, R., 2000. An Archaean arc basalt-Nb-enriched basalts-adakiteassociation: the 2.7 Ga Confederation assemblage of the Birch-Uchi greenstone belt, Superior Province. Contrib. Mineral. Petrol., 139: 208-226. 10.1007/PL00007672

Hollings, P. and Kerrich, R., 2006. Light rare earth element depleted to enriched basaltic flows from 2.8 to 2.7 Ga greenstone belts of the Uchi Subprovince, Ontario, Canada. Chem. Geol., 227 : 133-153. 10.1016/j.chemgeo.2005.09.010

Hollings, P., 2002. Archaean Nb-enriched basalts in the northern Superior Province. Lithos, 64: 1-14. 10.1016/S0024-4937(02)00154-8

Hussain, M.F., Mondal, M.E.A. and Ahmad, T., 2004. Petrological and geochemical characteristics of Archean gneisses and granitoids from Bastar craton, central India - implication for subduction related magmatism. Gondwana Research, 7: 531-537. 10.1016/S1342-937X(05)70803-0

Jayananda, M., Kano, T., Peucat, J.-J and Channabasappa, S., 2008. 3.35 Ga komatiite volcanism in the western Dharwar craton, southern India: Constraints from Nd isotopes and whole-rock geochemistry. Precambrian Research 162,160-179. 10.1016/j.precamres.2007.07.010

Kerr, A.C., 2004. Oceanic plateaus. Treatise Geochem., 3: 537-565.

Kerr, A.C. and Mahoney, J.J., 2007. Oceanic plateaus: problematic plumes, potential paradigms. Chem. Geol., 241: 332-353. 10.1016/j.chemgeo.2007.01.019

Manikyamba, C., Kerrich, R., Naqvi, S.M. and Mohan, M.R., 2004. Geochemical systematics of tholeiitic basalts from the 2.7 Ga Ramgiri-Hungund composite greenstone belt, Dharwar craton. Precam. Res., 134: 21-39. 10.1016/j.precamres.2004.05.010

Manikyamba, C. and Khanna, T.C., 2007. Crustal growth processes as illustrated by the Neoarchaean intracratonic magmatism from Gadwal greenstone belt, eastern Dharwar craton, India. Gondwans Res., 11 : 476-491. 10.1016/j.gr.2006.07.005

Mondal, M.E.A, Hussain, M.F and Ahmad, T., 2006. Continental Growth of Bastar Craton, Central Indian Shield during Precambrian via Multiphase Subduction and Lithospheric Extension/Rifting: Evidence from Geochemistry of Gneisses, Granitoids and Mafic dykes. Jour. Geosciences, 49 : 137-151.

Naqvi, S.M., Rogers, J.J.W., 1987. Precambrian Geology of India. Oxford University Press, New York, U.S.A.

Naqvi, S.M., Khan, R.M.K., Manikyamba, C., Mohan, M.R. and Khanna, T.C., 2006. Geochemistry of the Neoarchaean high-Mg basalts, boninites and adakites from the Kushtagi-Hungund greenstone belt of the eastern Dharwar craton; implications for the tectonic setting. Jour. Asian Earth Sci., 27:25-44. 10.1016/j.jseaes.2005.01.006

Patranabis-Deb, S, Bickford, M. E., Hill, B., Chaudhuri, A. K. and Basu, A., 2007. SHRIMP ages of zircon in the Uppermost tuff in Chattisgarh Basin in Central India require ~500-Ma adjustment in Indian Proterozoic stratigraphy. Jour. Geology, 115: 407-415.

Pearce, J., 1982. Trace element characteristics of lavas from the destructive plate boundaries. In: Trorpe, R.S. (Ed.) Andesites. John Wiley and Sons, pp. 525-548.

Pearce, J., 2003. Supra-subduction zone ophiolites: the search for modern analogues. In: Dilek, Y., Newcomb, S. (Eds.), Ophiolite Concept and the Evolution of Geological Thought. Geol. Soc. Am. Spec. Paper 373, pp. 269-293. 10.1130/0-8137-2373-6.269

Pearce, J.A., 2008. Geochemical fingerprinting of oceanic basalts with applications to ophiolite classification and the search for Archean oceanic crust. Lithos, 100: 14-48.

Polat, A., 2009. The geochemistry of Neoarchaean (ca. 2700 Ma) tholeiitic basalts, transitional to alkaline basalts, and gabbros, Wawa Subprovince: implications for petrogenetic and geodynamic processes. Precam. Res., 168: 83-105. 10.1016/j.precamres.2008.03.008

Polat, A., Kusky, T., Li, J., Fryer, B., Kerrich, R. and Patrick, K., 2005. Geochemistry of Neoarchaean (ca. 2.55- 2.50 Ga) volcanic and ophiolitic rocks of the Wutaishan belt, central orogenic belt, North China craton: implications for geodynamic setting and continental growth. Geol. Soc. Am. Bull., 117: 1378-1399. 10.1130/B25724.1

Polat, A. and Hofmann, A.W., 2003. Alteration and geochemical patterns in the 3.7-3.8 Ga Isua greenstone belt, West Greenland. Precam. Res., 126: 197-218. 10.1016/S0301-9268(03)00095-0

Pollard, P. J., Millburn, D., Taylor, R. G. and Cuff, C., 1983. Mineralogical and textural modifications in Granites associated with tin mineralisation, Herberton - Mt Garnet Tinfield, Queensland. In : Permian Geology of Queensland, Brisbane. Geol. Soc. Australia, Queensland Div. pp. 413-430.

Prasad, B., 1990. Observations in the Precambrian geology of Central India vis a vis adjoining region. Geol. Surv. India, Special Pub. 28, 181 - 198.

Puchtel, I.S., Hofmann, A.W., Amelin, Yu. V.; Garbe-Schonberg, C.D.; Samsonov, A.V. and Shchipansky, 1999. Combined mantle plume-island arc model for the formation of the 2.9 Ga Sumozero-Kenozero greenstone belt, SE Baltic shield: isotope and trace element constraints. Geochim Cosmochim Acta 63: 3579-3595.

Ramakrishnan, M., 1990. Crustal development in Southern Bastar, Central Indian craton. Geol. Surv. India Special Pub. 28, 44 - 66.

Redman, B.A. and Keys, R.R., 1985. Archaean basic volcanism in the eastern Goldfields province, Yilgarn Block, western Australia. Precam. Res., 30: 113-152. 10.1016/0301-9268(85)90048-8

Roeder, P.L. and Emsile, R.F., 1970. Olivine - liquid equilibrium. Contrib. Min. Petrol., 29:275-289. 10.1007/BF00371276

Roy, P., Balaram, V., Kumar, A., Satyanarayanan, M. and Gnaneshwar Rao, T., 2007. New REE and trace element data on two kimberlitic reference materials by ICP-MS. Geostandard and Geoanalytical Research, 31:261-273. 10.1111/j.1751-908X.2007.00836.x

Saha, D., Deb, G.K. and Dutta, S., 2000. Granite-greenstone relationship in the Sonakhan belt, Raipur district, central India. Geol. Surv. India Special Pub. No. 57 : 67-78.

Sanderman, H.A., Hammer, S., Davis, W.J., Ryan, J.J. and Peterson, T.D., 2004. Neoarchaean volcanic rocks, Central Hearne supracrustal belt, Western Churchill Province, Canada: geochemical and isotopic evidence supporting intra-oceanic, suprasubduction zone extension. Precam. Res., 134: 113-141. 10.1016/j.precamres.2004.03.014

Sandeman, H.A., Hanmer, S., Tella, S., Armitage, A.A., davis, W.J. and Ryan, J.J., 2006. Petrogenesis of Neoarchaean volcanic rocks of the MacQuoid supracrustal belt: a back-arc setting for the northwestern Hearne subdomain, western Churchill Province, Canada. Precam. Res., 144:14-165.

Stein M. and Goldstein, S.L., 1996. From plume head to continental lithosphere in the Arabian-Nubian shield. Nature, 382: 773-778. 10.1038/382773a0

Stein, H.J., Hannah, J.L., Zimmerman, A., Markey, R.J., Sarkar, S.C. and Pal, A.B., 2004. A 2.5 Ga porphyry Cu-Mo-Au deposit at Malanjkhand, central India: implications for late Archaean continental assembly. Precam. Res., 134: 189-226. 10.1016/j.precamres.2004.05.012

Srivastava, R.K.and Verma, R., 1998. Precambrian basic magmatism of the southern Bastar craton, central India. In: Paliwal, B.S. (Ed.), The Indian Precambrian, Scientific Publication, India, pp. 409-416.

Srivastava, R.K. and Singh, R.K., 1999. Petrology and geochemistry of the late Archaean siliceous high-magnesian basalts (SHMB) from Kaklur, southern Bastar craton, central India. Jour. Geol. Soc. India, 53 : 693-704.

Srivastava, R.K., Singh, R.K., Verma, S.P., 2004. Neoarchean mafic volcanic rocks from the southern Bastar greenstone belt, Central India: petrological and tectonic significance. Precambrian Res. 131, 305 - 322. 10.1016/j.precamres.2003.12.013

Srivastava, R.K., Ellam, R.M. and Gautam, G.C, 2009. Sr-Nd isotope geochemistry of the early Precambrian sub-alkaline mafic igneous rocks from the southern Bastar craton, Central India. Miner Petrol, 96:71-79.

Sun, S.S., McDonough, W.F., 1989. Chemical and Isotopic systematics of oceanic basalts: implications for mantle composition and processes. In: A.D. Saunder and M.J Norry (eds.), Magmatism in oceanic basins Geol. Soc. London Special Pub. 42, 313 - 345.

Taylor, R. G. and Pollard P. J., 1988. Pervasive hydrothermal alteration in tin bearing granites and implications for the evolution of ore-bearing fluids. In: Taylor, R. P. and Strong D. F. (Eds.), Recent advances in the Geology of the Granite related mineral deposits. Canadian Institute of Mining and Metallurgy, Quebec, pp. 86-95.

Van Boening, A.M. and Nabelek, P.I., 2008. Petrogenesis and tectonic implications of Paleoproterozoic mafic rocks in the Black Hills, South Dakota. Precam. Res., 167: 363-376. 10.1016/j.precamres.2008.09.008

Winchester, J. A. and Floyd, P. A., 1977. Geochemical discrimination of different magma series and their differentiation products using immobile elements. Chemical Geology, 20: 325-343. 10.1016/0009-2541(77)90057-2

Wyman, D.A., Ayer, J.A and Devaney, J.R., 2000. Niobium-enriched basalts from the Wabigoon subprovince, Canada: evidence for adakitic metasomatism above an Archaean subduction. Earth Planet. Lett., 179 : 21-30. 10.1016/S0012-821X(00)00106-0